A Chemically Synthesized Version of the Insect Antibacterial Glycopeptide, Diptericin, Disrupts Bacterial Membrane Integrity†

Katharine A. Winans,‡ David S. King,§ Vikram R. Rao,‡ and Carolyn R. Bertozzi*,‡

Department of Chemistry and Howard Hughes Medical Institute, University of California, Berkeley, California 94720

Received June 2, 1999; Revised Manuscript Received July 15, 1999

ABSTRACT: Insects protect themselves against bacterial infection by secreting a battery of antimicrobial peptides into the hemolymph. Despite recent progress, important mechanistic questions, such as the precise bacterial targets, the nature of any cooperation that occurs between peptides, and the purpose of multiple peptide isoforms, remain largely unanswered. We report herein the chemical synthesis and preliminary mechanistic investigation of diptericin, an 82 residue glycopeptide that contains regions similar to two different types of antibacterial peptides. A revised, highly practical synthesis of the precursor N^{α}-Fmoc-Thr(Ac_3-α-D-GalNAc) allowed us to produce sufficient quantities of the glycopeptide for mechanistic assays. The synthetic, full-length polypeptide proved to be active in growth inhibition assays with an IC_{50} of approximately 250 nM, a concentration similar to that found in the insect hemolymph. Biological analysis of diptericin fragments indicated that the main determinant of antibacterial activity lay in the C-terminal region that is similar to the attacin peptides, although the N-terminal segment, related to the proline-rich family of antibacterial peptides, augmented that activity by 100-fold. In all assays, activity appeared glycosylation independent. Circular dichroism of unglycosylated diptericin indicated that the peptide lacked structure both in plain buffer and in the presence of liposomes. Diptericin increased the permeability of the outer and inner membranes of *Escherichia coli* D22 cells, suggesting possible mechanisms of action. The ability to access glycopeptides of this type through chemical synthesis will facilitate further mechanistic studies.

Insects rely on a simple but remarkably effective immune strategy. Bacterial infection is greeted by two types of responses: a cellular defense in which microbes are phagocytosed or encapsulated by hemocytes (the insect equivalent of blood cells) and a humoral defense in which an array of antibacterial peptides is secreted *en masse* into the hemolymph (reviewed in (*2*) and (*3*)). There is little specificity encoded in the defense; unrelated microbes or even physical injury elicits the same battery of peptides. Furthermore, this rapid response, which may last up to several days, exhibits no memory for previous immunological insults. These observations could class the insect strategy as a crude assault rather than a finely orchestrated offensive. Yet these antibiotics have succeeded in protecting insects from bacterial pathogens for millions of years, whereas our clinical attempts to treat infectious disease in the past several decades have yielded a generation of multidrug resistant microbes. In the search for strategies that circumvent drug resistance, a more thorough consideration of insect antibacterial peptides may be warranted.

Research begun in the 1970s by Hans Boman and expanded upon since by many others has illuminated the peptides' fundamental characteristics (*2*, *3*). Several categories have been identified: lysozymes, cecropins, defensins, attacins, and proline-rich peptides. An additional class, the diptericins, contains sequence elements similar to both of the latter two categories. So far, the common bacterial target appears to be the cell envelope; however, mechanisms of attack vary widely and, in some cases, are partly or completely unexplored. The simultaneous release of many peptides upon bacterial infection suggests that their antibacterial activities may be complementary to each other, the peptides working synergistically to disable bacteria. Indeed, a hybrid of cecropin and the cytolytic peptide melittin that disrupts the bacterial membrane has been shown to potentiate the antibacterial activity of lysozyme, which cleaves the sugar backbone of peptidoglycan (*4*). More subtle manifestations of this theme remain to be elucidated. Finally, many antibacterial peptides are secreted into the hemolymph in several isoforms that are generated by differential proteolysis or glycosylation or by gene duplications (*3*, *5*). While the purpose of these alterations is largely unknown, glycosylation does modulate antibacterial potency in some cases (*6*, *7*). A full understanding of how the network of antibacterial peptides operates will require an examination of the range and potency of each isoform's activity.

† The authors acknowledge funding from the Arnold and Mabel Beckman Foundation, the W.M. Keck Foundation, Glaxo Wellcome, the Burroughs Wellcome Fund and the Camille and Henry Dreyfus Foundation. V.R.R. was supported by an award from the Beckman Scholars Program. Some mass spectra were obtained at the UCSF Mass Spectrometry Facility (A.L. Burlingame, Director) supported by the Biomedical Research Technology Program of the National Center for Research Resources (NIH NCRR BRTP 01614). This research was supported by grants to C.R.B. from the National Science Foundation (CHE-9734430) and the University of California BioSTAR Project (S97-73).

* To whom correspondence should be addressed. Telephone: 510-643-1682. Fax: 510-643-2628. E-mail: bertozzi@cchem.berkeley.edu.

‡ Department of Chemistry.

§ Howard Hughes Medical Institute.

10.1021/bi991247f CCC: $18.00
Published on Web 08/14/1999

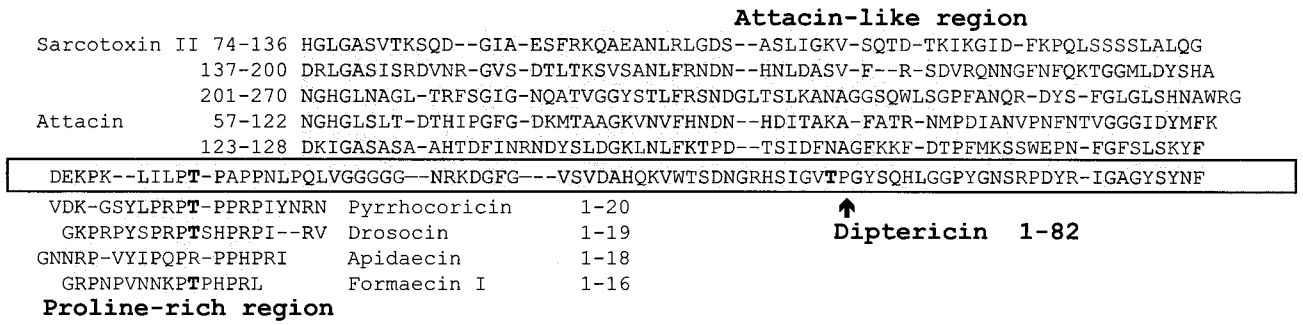

FIGURE 1: Sequence comparison of diptericin from *Phormia terranovae* with members of the proline-rich and attacin-like peptide families, adapted in part from Hultmark (2). Sequence identities and conservative substitutions are shaded. Numbers to the right of peptide names indicate the positions of amino acid residues in the mature peptides. Known sites of threonine-linked glycosylation are noted in boldface (**T**). The peptides included follow: *Hyalophora cecropia* acidic attacin (54, 55), *Sarcophaga peregrina* sarcotoxin IIA (56), *Phormia terranovae* diptericin (5), *Pyrrhocoris apterus* pyrrhocoricin (57), *Drosophila melanogaster* drosocin (6), *Apis mellifera* apidaecin (58), and *Myrmecia gulosa* formaecin I (50).

We have chosen to study the diptericins, a particularly intriguing category of antibacterial peptides. Homologues have been identified in *Phormia terranovae*, *Drosophila melanogaster*, and *Sarcophaga peregrina*; our studies focus on the *Phormia* version and subsequent allusions to diptericin refer to that sequence (reviewed in (*8*)). Diptericin is unique among the antibacterial peptides in that it bears a modular structure, with sequence elements of both the proline-rich peptides and the attacins (Figure 1) (*5*). Neither the evolutionary rationale for this design nor the means by which diptericin acts is understood. Available information suggests that attacins compromise membrane integrity by inhibiting the synthesis of outer membrane proteins without actually entering the bacterial cell (*9*−*11*). Proline-rich peptides are believed to target specific bacterial receptors, as opposed to interacting in a nonspecific way with membranes since the all-D-amino acid versions of two members of this class are markedly reduced in activity (*12*, *13*). For both classes of peptides, precise mechanistic details are lacking. While little is known about diptericin itself, one study has suggested that it targets the bacterial inner membrane (*14*). Studies of diptericin may provide insight into all three types of antibacterial peptides. Further, such studies may suggest how cooperative activity between antibacterial peptides is achieved.

Diptericin, subject to an additional layer of structural complexity, boasts two sites of O-linked glycosylation: threonines 10 and 54 (Figure 1). The peptide is secreted into the hemolymph in a variety of glycoforms with carbohydrates ranging from mono- to trisaccharides at each glycosylation site; these modifications are reportedly required for activity (*5*). The simplest isoform bears a single GalNAc[1] residue at one site and retains antibacterial activity. Since the location of the solitary GalNAc residue has not been assigned, we chose the better defined isoform bearing GalNAc residues at both threonines 10 and 54 as our preliminary target; according to the previous report, the antibacterial potencies of the two versions are almost identical. We hypothesize that an analysis of glycosylation's role in this system may offer clues as to the broader role that antibacterial peptide isoforms play in the insect defense.

A challenging aspect of our study was the production of significant quantities of glycosylated diptericin. Protein expression in *Escherichia coli* or eukaryotic cultured cells is now routine, but unfortunately, such procedures were inappropriate for our studies. Because the efficiency of glycosylating enzymes in a eukaryotic cell's secretory apparatus varies, a mixture of oligosaccharide structures at any glycosylation site is possible. The result would be a heterogeneous pool of diptericin glycoforms unsuitable for the experiments we planned. We circumvented these problems by chemically synthesizing diptericin, using an extension of techniques applied previously to the synthesis of short glycopeptides (*15*−*20*). This approach allowed us to produce a specific glycoform as well as to synthesize fragments of the larger protein that would permit us to probe the independent activities of its two "domains." We report herein the total chemical synthesis of glycosylated diptericin and fragments derived from it. Our results show that this chemically synthesized version is biologically active at concentrations found in insect hemolymph. Mechanistic assays suggest that one component of the antibacterial activity is to increase the permeability of the bacterial inner and outer membranes and that the major determinant of this activity lies in the C-terminal attacin-like region of the peptide.

MATERIALS AND METHODS

General Methods. All chemical reagents were obtained from commercial suppliers and used without further purification. The following solvents were distilled under a nitrogen atmosphere prior to use: THF was dried and deoxygenated over Na and benzophenone; CH_2Cl_2 and CH_3CN were dried over CaH_2; toluene was dried over Na. Unless otherwise noted, all air and moisture sensitive reactions were performed under an argon atmosphere. Analytical thin-layer chromatography (TLC) was conducted on Analtech Uniplate silica gel plates with detection by ceric ammonium molybdate (CAM) and/or by UV light. For flash chromatography, 60 Å silica gel (Bodman) was employed. Reversed-phase high-pressure liquid chromatography (RP-HPLC) was performed on a Rainin Dynamax SD-200 system using Microsorb and

[1] Abbreviations: CAM, ceric ammonium molybdate; CAN, ceric ammonium nitrate; CD, circular dichroism; DCC, *N*, *N*′-dicyclohexylcarbodiimide; GalNAc, *N*-acetylgalactosamine; HBTU, 2-(1H-benzotriazole-1-yl)-1,1,3,3-tetramethyluronium hexafluorophosphate; HOBt, *N*-hydroxybenzotriazole; LB, Luria-Bertani media; MBHA, 4-methylbenzylhydrylamine; NMP, 1-methyl-2-pyrrolidinone; ONPG, *o*-nitrophenyl-*β*-D-galactopyranoside; RP-HPLC, reversed phase high-pressure liquid chromatography; TFA, trifluoroacetic acid; THF, tetrahydrofuran; TLC, thin-layer chromatography.

Dynamax C_{18} reversed-phase columns (analytical: 4.6 mm ID × 25 cm, 1 mL/min; semipreparative: 10 mm ID × 25 cm, 4 mL/min) and UV detection (230 nm) was performed with a Rainin Dynamax UV-1 detector.

The ^{1}H and ^{13}C NMR spectra were obtained with Bruker AMX-300 and AMX-400 spectrometers. Chemical shifts are reported in δ values downfield from tetramethylsilane, and coupling constants are reported in Hz. Electrospray ionization mass spectrometry (ESI-MS) was performed at the University of California, San Francisco Mass Spectrometry Facility on a Sciex 300 Electrospray mass spectrometer and at the University of California, Berkeley on a Hewlett-Packard 5989A mass spectrometer or a Bruker Esquire-LC electrospray ion trap mass spectrometer.

Bacterial Strains. The *E. coli* strain D22 used in bacterial assays was obtained from the *E. coli* Genetic Stock Center at Yale University (*http://cgsc.biology.yale.edu)*. The *E. coli* strain ML-35 was a gift of Professor Robert E. W. Hancock of the University of British Columbia.

*3,4,6-Tri-O-acetyl-D-galactal (**3**) (21, 22).* Zinc dust (98.0 g, 1.50 mol) was added to 500 mL of 1:1 AcOH/H_2O that was being vigorously stirred with an overhead stirrer at 4 °C. A solution of 68.8 g (0.167 mol) of crude 2,3,4,6-tetra-*O*-acetyl-α-D-galactopyranosyl bromide (**2**) (*23*, *24*) was dissolved in 500 mL of ether and added dropwise via an addition funnel over a 1 h period. The reaction was allowed to stir overnight (approximately 15 h), during which time it warmed to room temperature. The reaction progress was monitored by ^{1}H NMR. The ether phase was collected and the aqueous layer extracted with ether (6 × 50 mL). Repeated rinsing of the zinc dust with ether was required to recover all of the product. The combined ether layers were washed with saturated $NaHCO_3$ (15 × 100 mL), which was accompanied by vigorous CO_2 evolution. Combined aqueous layers were extracted with ether (8 × 50 mL). Ether layers were again pooled and washed with H_2O (2 × 200 mL) and brine (1 × 200 mL); these aqueous layers were extracted with ether (6 × 50 mL and 4 × 50 mL, respectively). Finally, the ether solution was dried over Na_2SO_4 and concentrated in vacuo, yielding 44.6 g (98%) of a clear syrup. Typical yields for this reaction range from 90 to 98%. This compound was judged sufficiently pure by ^{1}H NMR analysis to be carried on without further purification. ^{1}H NMR (300 MHz, $CDCl_3$): δ 2.02 (s, 3H), 2.08 (s, 3H), 2.13 (s, 3H), 4.18−4.34 (m, 3H), 4.73 (ddd, 1H, J = 6.4, 2.6,1.5), 5.41−5.44 (m, 1H), 5.54−5.57 (m, 1H), 6.46 (dd, 1H, J = 1.7, 6.3).

*2-Azido-2-deoxy-3,4,6-tri-O-acetyl-D-galactopyranosyl nitrate (mixture of anomers) (**4**) (25).* Tri-*O*-acetyl galactal (**3**) (44.0 g, 0.162 mol) was dissolved in 550 mL of CH_3CN and cooled to −15 °C, while being stirred with an overhead stirrer. After 10 min, 275 g (0.501 mol) of ceric ammonium nitrate (CAN) and 16.3 g (0.251 mol) of sodium azide were added. The reaction, stirred vigorously, was kept at −15 °C for about 7 h but was allowed to warm to room temperature overnight. The reaction progress was monitored by TLC (1:1 hexanes/ethyl acetate, stained with CAM), the azidonitrate boasting a slightly higher R_f than the starting material. The reaction was terminated at 18 h. The mixture was diluted with 300 mL of ether, and this solution was washed with H_2O (6 × 100 mL). The aqueous layers were extracted with ether (8 × 50 mL) to recover residual product. Ether layers were pooled and dried over Na_2SO_4, then concentrated in vacuo to afford a yellow syrup. Purification by silica gel chromatography eluting with 3:1 hexanes/ethyl acetate gave 23.0 g (38%) of an off-white solid as a mixture of anomers. Characteristic peaks in the ^{1}H NMR spectrum (400 MHz, $CDCl_3$): δ 6.33 (H-1, α) (d, 1H, J = 4.3) and 5.56 (H-1, β) (d, 1H, J = 8.8).

*2-Azido-2-deoxy-3,4,6-tri-O-acetyl-α-D-galactopyranosyl bromide (**5**) (25).* To a solution of 10.0 g of azidonitrate **4** (27 mmol) in 89 mL of CH_3CN was added LiBr (11.5 g, 133 mmol). The reaction was stirred at room temperature for 4 h. The reaction progress was best monitored by ^{1}H NMR analysis. The solution was diluted with 300 mL of chilled CH_2Cl_2, and this organic phase was washed with cold H_2O (4 × 60 mL). Aqueous layers were extracted with CH_2Cl_2 (3 × 50 mL) until they contained no product. The organic layers were pooled and dried over Na_2SO_4, then concentrated in vacuo to afford a yellow syrup (10.1 g, 95%). By ^{1}H NMR analysis, this product was judged to be sufficiently pure for use in subsequent steps. ^{1}H NMR (300 MHz, $CDCl_3$): δ 2.06 (s, 3H), 2.07 (s, 3H), 2.16 (s, 3H), 3.99 (dd, 1H, J = 3.8, 10.7), 4.46−4.51 (m, 1H), 5.35 (dd, 1H, J = 3.2, 10.7), 5.51 (dd, 1H, J = 1.4, 3.2), 6.47 (d, 1H, J = 3.8).

*N^{α}-(Fluoren-9-ylmethoxycarbonyl)-O-(3,4,6-tri-O-acetyl-2-azido-2-deoxy-α-D-galactopyranosyl)-L-threonine benzyl ester (**7**) (26).* With the exclusion of light and moisture, a solution of N^{α}-(fluoren-9-ylmethoxycarbonyl)-L-threonine benzyl ester (**6**) (*27*) (2.0 g, 4.6 mmol), Ag_2CO_3 (3.6 g, 13.8 mmol), and 4 Å molecular sieve dust (2.0 g) in 23 mL of 1:1 CH_2Cl_2/toluene was stirred at room temperature for 45 min. $AgClO_4$ (1.2 g, 4.6 mmol) was added, and the reaction was stirred for another 20 min. A solution of azidobromide **5** (3.3 g, 8.4 mmol) in 23 mL of 1:1 CH_2Cl_2/toluene was added via syringe over a 30 min period. After 4 d, the mixture was filtered over Celite, with additional CH_2Cl_2 used to rinse the Celite until no product was retained. The filtrate was diluted with CH_2Cl_2 to about 200 mL and then washed with saturated $NaHCO_3$ (3 × 50 mL) and H_2O (2 × 50 mL). All aqueous washes were back-extracted with CH_2Cl_2. The pooled organic layers were dried over Na_2SO_4 for 1 h and then concentrated in vacuo. The desired α-glycoside product was difficult to separate from unreacted starting material by chromatography; thus, the crude residue (3.4 g) was taken directly on to the next step. Characteristic peaks in the ^{1}H NMR (400 MHz, $CDCl_3$): δ 1.35 (d, 3H, J = 6.2, Thr-CH_3), 3.59 (dd, 1H, J = 3.7, 11.2, H-2), 4.91 (d, 1H, J = 3.7, H-1), 5.45 (app s, 1H, H-4), 5.70 (d, 1H, J = 9.4, Thr-NH).

*N^{α}-(Fluoren-9-ylmethoxycarbonyl)-O-(2-acetamido-2-deoxy-3,4,6-tri-O-acetyl-α-D-galactopyranosyl)-L-threonine benzyl ester (26) (**8**).* To a solution of crude **7** (3.4 g) in 150 mL of THF/Ac_2O/AcOH (3:2:1) was added zinc dust (3.94 g, 60.3 mmol); 7.5 mL of saturated aqueous $CuSO_4$, added last, served to activate the zinc. The reaction, monitored by TLC (1:1.5 hexanes/ethyl acetate), was complete within 10 min. The reaction mixture was filtered through Celite and the filtrate concentrated in vacuo by coevaporation with toluene. Purification by silica gel chromatography eluting with 1:1 hexanes/ethyl acetate gave 2.3 g (64% over two steps) of a white, foamy glass. Characteristic peaks in the ^{1}H NMR (400 MHz, $CDCl_3$): δ 1.30 (d, 3H, J = 6.3, Thr-CH_3), 4.79 (d, 1H, J = 3.4, H-1), 5.37 (app s, 1H, H-4), 5.58 (d, 1H, J = 9.5, Thr-NH), 5.75 (d, 1H, J = 9.5, AcNH).

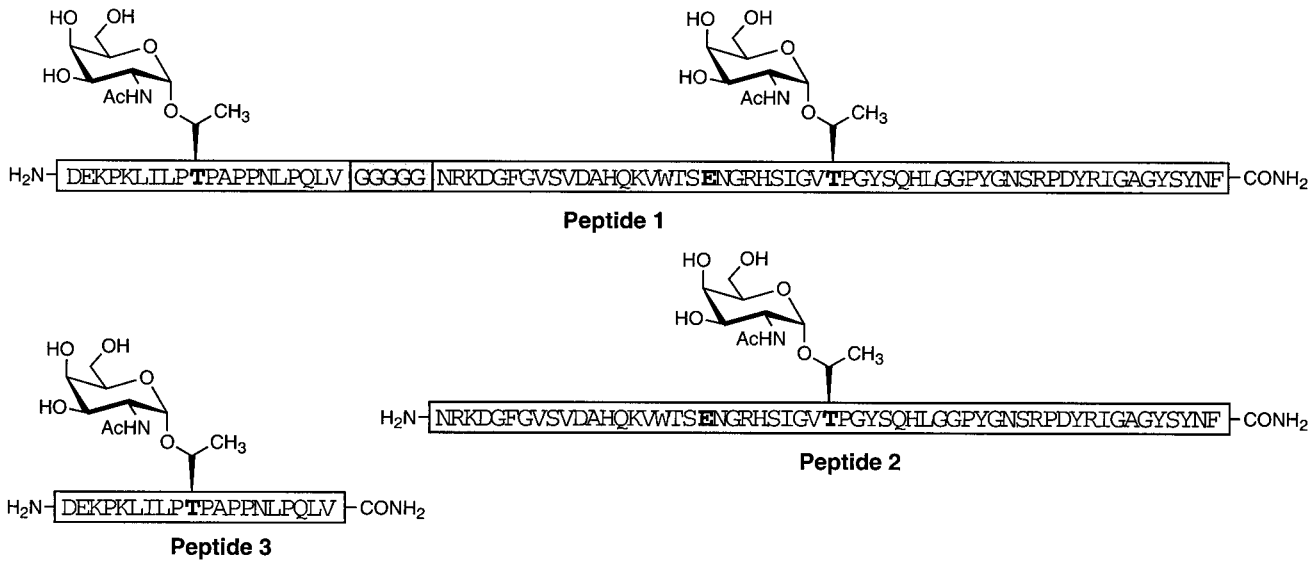

FIGURE 2: Diptericin peptides synthesized. The following constructs were synthesized as described in the text: the full-length, 82 residue glycopeptide (Peptide 1); the 57 residue, glycosylated, attacin-like fragment (Peptide 2); and the 20 residue, glycosylated, proline-rich fragment (Peptide 3). Each peptide was synthesized as well in its unglycosylated form (referred to as Peptides 4, 5, and 6, respectively, in the subsequent text). The boldface **E** in the attacin-like regions of the peptides denotes the site of an Asp→Glu mutation (see text for further explanation).

N$^{\alpha}$*-(Fluoren-9-ylmethoxycarbonyl)-O-(2-acetamido-2-deoxy-3,4,6-tri-O-acetyl-*α*-D-galactopyranosyl)-L-threonine (**1**) (19, 20).* To a solution of benzyl ester **8** (2.3 g, 3.0 mmol) in 80 mL of methanol was added 10% Pd/C (approximately 0.3 g); H_2 was then bubbled through the reaction mixture. Monitored by TLC (6:1 chloroform/methanol), the reaction was complete within 20 min. The mixture was filtered through Celite to remove the Pd/C, with copious rinsing with methanol to remove all product from the solids. The crude product was concentrated in vacuo and purified by silica gel chromatography, eluting with 10:1 chloroform/methanol (0.5% AcOH) to yield 1.2 g of a white solid (60%). Purification was often unnecessary as the other product, toluene, was easily removed by evaporation. ^{1}H NMR (300 MHz, CD_3OD): δ 1.22 (d, 3H, $J = 6.4$), 1.93 (s, 3H), 1.96 (s, 3H), 2.01 (s, 3H), 2.11 (s, 3H), 4.03−4.10 (m, 3H), 4.23 (app t, 1H, $J = 6.3$), 4.28−4.41 (m, 4H), 4.54 (dd, 1H, $J =$ 6.6, 10.7), 5.06 (d, 1H, $J = 4.1$), 5.11 (dd, 1H, $J = 11.6$, 3.2), 5.39 (app d, 1H, $J = 2.5$), 7.28−7.81 (m, 8H).

Peptide Synthesis. Diptericin constructs were synthesized on Rink amide MBHA resin (Novabiochem) using *N*$^{\alpha}$-Fmoc-protected amino acids and DCC-mediated HOBt ester activation in NMP (ABI 431A synthesizer, user-devised cycles). For glycosylated constructs, the glycosylated amino acid *N*$^{\alpha}$-Fmoc-Thr(Ac_3-α-D-GalNAc) (**1**) was hand-coupled, using 2.5 equiv of amino acid and activation with HBTU (2 equiv) in the presence of HOBt and *N*,*N*-diisopropylethylamine (2 equiv each); typical reaction time was 1.5 h. The efficiency of acylation appeared to vary with the peptide sequence; for some locations, up to three coupling reactions were necessary to maximize the yield of the glycosylated product. Peptide cleavage/deprotection was accomplished with Reagent K (3.5 h, rt) (*28*); for the constructs 57 and 82 amino acids in length, deprotection with Reagent K was repeated. Purification was accomplished via RP-HPLC, eluting with a gradient of 10−50% acetonitrile in water, both containing 0.1% (vol/vol) trifluoroacetic acid (TFA). Estimated yields based on the molar equivalents of resin used for each synthesis were as follows (carbohydrate residues remained acetylated at this stage): Peptide 1, 3.5%; Peptide 2, 9.7%; Peptide 3, 60%; Peptide 4, 16%; Peptide 5, 23%; Peptide 6, 70%. Purified glycopeptides were treated with 5% hydrazine hydrate in H_2O to deacetylate the sugar moieties; reactions were monitored by RP-HPLC and were complete in times ranging from 15 min to 1 h. These completely deprotected glycopeptides were again purified by RP-HPLC. Yields for deacetylation reactions ranged from 60 to 80%. The products were analyzed by ESI-MS. Peptide 1 (as described in Figure 2): calcd 9112.0, found 9112.0. Peptide 2: calcd 6460.9, found 6460.8. Peptide 3: calcd 2382.8, found 2382.2. Peptide 4: calcd 8705.7, found 8705.6. Peptide 5: calcd 6257.8, found 6258.1. Peptide 6: calcd 2179.6, found 2179.4.

Peptide Stock Solution Preparation. Peptide concentrations were determined by calculating the molar extinction coefficient (*29*), measuring the $A_{276\ nm}$ of a stock solution and finally calculating the concentration using Beer's law: for Peptide 4 (full-length diptericin), $\epsilon_{276\ nm}(H_2O) = 11\ 814\ M^{-1}\ cm^{-1}$, for Peptide 5 (the attacin-like fragment), $\epsilon_{276\ nm}(H_2O) = 12\ 351\ M^{-1}\ cm^{-1}$. The extinction coefficients calculated for unglycosylated peptides were used for their glycosylated counterparts. In the case of Peptides 3 and 6 (the proline-rich fragments), since no aromatic amino acids were present such calculations were not applicable. In this case, peptide concentrations were measured after repeated dissolving of the peptide sample in water followed by lyophilization to remove the maximum amount of TFA. The concentration was determined by taking a dry weight measurement and assuming that 80% of that weight was peptide, and the remainder residual water and TFA salt. Final concentrations ranged from 10^{-10} to 10^{-3} M; the precise range used for a given peptide depended on its potency.

Lipid Vesicle Preparation. Powdered 1,2-dimyristoyl-sn-glycero-3-phosphocholine or 1,2-dimyristoyl-sn-glycero-3-phosphoglycerol (Avanti Polar Lipids; Alabaster, AL) was dissolved in a minimal volume of 6:1 chloroform/methanol

(vol/vol) and evaporated to dryness on the sides of a test tube. A volume of 10 mM potassium phosphate (pH 7.0) calculated to generate a 6 mM solution of lipid was added. The solution was sonicated for approximately 30 min, until the initially cloudy suspension became clear. This stock solution was diluted with potassium phosphate to 3 mM; serial dilutions yielded solutions at 0.3 and 0.03 mM lipid. These three liposome solutions were used immediately in circular dichroism (CD) experiments; stock solutions of unglycosylated diptericin (Peptide 4) at 600 μM were diluted 100-fold with the liposome solutions, and CD spectra were acquired as described below.

Circular Dichroism Spectroscopy. Far-UV CD spectra of full-length diptericin (Peptide 4) were recorded on an Aviv Model 62 DS spectropolarimeter at 25 °C. Wavelength scans from 200 to 300 nm were measured at 1 nm intervals with a 1.5 nm bandwidth and a 1 s averaging time. Each scan was repeated three times and averaged. The appropriate background of buffer or liposome was subtracted from each spectrum. The mean residue molar ellipticity $[\theta]$ (deg cm^2 dmol^{-1}) was calculated from the equation $[\theta] = 100\ \theta/(lcn)$, where θ is the measured ellipticity in millidegrees, c is the concentration of peptide in millimolar, l is the path length of the cell in centimeters, and n is the number of amino acid residues in the peptide.

Bacterial Growth Inhibition Assays. Growth inhibition assays were performed in 96-well microtiter plates (Corning Costar, half area wells) with a final volume of 55 μL per well; bacterial growth was monitored by the change in $OD_{415\ nm}$, which we have found is directly correlated with the density of viable cells (data not shown). The 55 μL volume was comprised of 50 μL of bacterial culture (described below) added to 5 μL of serially diluted peptide. The bacterial culture was prepared by growing *E. coli* D22 cells in Luria−Bertani (LB) media containing streptomycin (50 μg/mL) to mid-logarithmic phase, then diluting with LB/streptomycin to $A_{415} = 0.01$ (absorbance of a 50 μL sample in one well of a 96-well microtiter plate). Plates were incubated for 24 h at 25 °C with periodic shaking. Growth was monitored by measuring $OD_{415\ nm}$ on a BioRad 550 microtiterplate reader; ΔOD values reported are calculated by subtracting $OD_{415\ nm}$ at $t = 0$ h from $OD_{415\ nm}$ at $t = 24$ h. For viable cell count experiments, aliquots of these cultures were withdrawn, diluted in LB, and plated on LB plates containing streptomycin (50 μg/mL).

Assay for Outer Membrane Integrity. Assays were performed in 96-well microtiter plates (Corning Costar, half area wells), with a total volume of 100 μL per well. The density of viable bacteria was monitored by the $OD_{415\ nm}$. In the assay, 80 μL of a diluted log-phase culture of *E. coli* D22 (as described for the growth inhibition assay) was added to 10 μL of peptide stock solution, polymyxin B, or water (2.5 μM stock solution for full-length diptericin, 250 μM for the attacin-like fragments, 1 mM for the proline-rich fragments, 1.0 μM for polymyxin B (Sigma, P-1004). Plates were incubated at 25 °C until reasonable growth was observed (approximately 7 h). At that time, 10 μL of a 2 mg/mL solution of chicken egg white lysozyme (Sigma, L-7651) was added. ΔOD values reported are calculated by subtracting $OD_{415\ nm}$ at $t = 0$ h from $OD_{415\ nm}$ at each time point.

Assay for Inner Membrane Integrity. Assays were performed using a procedure derived from Falla et al. (*30*). A suspension of *E. coli* ML-35 cells was prepared as follows: 1 mL of a saturated culture of ML-35 cells in LB broth was used to inoculate 50 mL of LB. The culture was incubated at 37 °C until the $OD_{595\ nm}$ of a 1 mL aliquot reached 0.5 (1.75 h). The cells were pelleted at room temperature, resuspended in 45 mL of 10 mM sodium phosphate (pH 7.4), and repelleted. According to Falla, it was important to pellet the cells at room temperature as bacteria could become leaky at colder temperatures. The pellet was resuspended in 20 mM sodium phosphate (pH 7.4) to a final $OD_{580\ nm}$ of 1.0.

A 96-well microtiter plate was loaded with 10 μL aliquots of antibiotic or peptide stock solutions (10 μM) or water. The bacterial suspension described above was mixed with an equal volume of 3 mM *o*-nitropheny-β-D-galactopyranoside (ONPG, Sigma N-1127) in water, and 90 μL aliquots were combined with peptide solutions to yield a total volume of 100 μL per well. The cleavage of ONPG by β-galactosidase was monitored as the change in $OD_{415\ nm}$; readings were recorded immediately after addition of the bacterial suspension. ΔOD values reported are calculated by subtracting $OD_{415\ nm}$ at $t = 0$ h from $OD_{415\ nm}$ at each time point. The ΔOD of a control well containing water instead of peptide solution was taken as background and was subtracted from other ΔOD values.

RESULTS

Chemical Synthesis of Diptericin and Putative Domains. To assess the role of glycosylation in diptericin's antibacterial activity, as well as analyze the respective contributions of the amino-terminal proline-rich region and carboxy-terminal attacin-like region, we synthesized the constructs shown in Figure 2. We posited that the stretch of five glycine residues from positions 21 through 25 of diptericin (the darkly shaded region of Peptide 1 in Figure 2) might function as a flexible linker between the domains; we chose to omit this putative linker from the diptericin fragments, Peptides 2, 3, 5, and 6.

The key challenge in our chemical synthesis of diptericin was installation of the two GalNAc residues into the protein sequence. Our strategy followed a method used routinely in O-linked glycopeptide synthesis (*15*−*20*). A glycosylated amino acid (compound **1** in Figure 3) was incorporated into the sequence via solid-phase peptide synthesis. Separate rounds of peptide deprotection and carbohydrate deacetylation—each followed by HPLC purification—yielded the final glycopeptide products shown in Figure 2. While the synthesis of the critical building block **1** had been accomplished by a variety of strategies ((*19*, *20*), reviewed in (*31*, *32*))—indeed, it was commercially available, albeit prohibitively expensive—we desired a route that was amenable to large scale production of this important precursor. We thus developed the scheme depicted in Figure 3, which assimilated and modified several previously reported reactions to allow multigram production of **1** with relative ease. Critical to the utility of this scheme were a number of high-yielding steps that allowed product to be carried forward without intervening purification. The galactosyl bromide **2** (*23*), which was readily prepared from free galactose in two quantitative steps, was used crude in a zinc-mediated reduction to form galactal **3**. We found that triphasic reaction conditions (Zn dust/

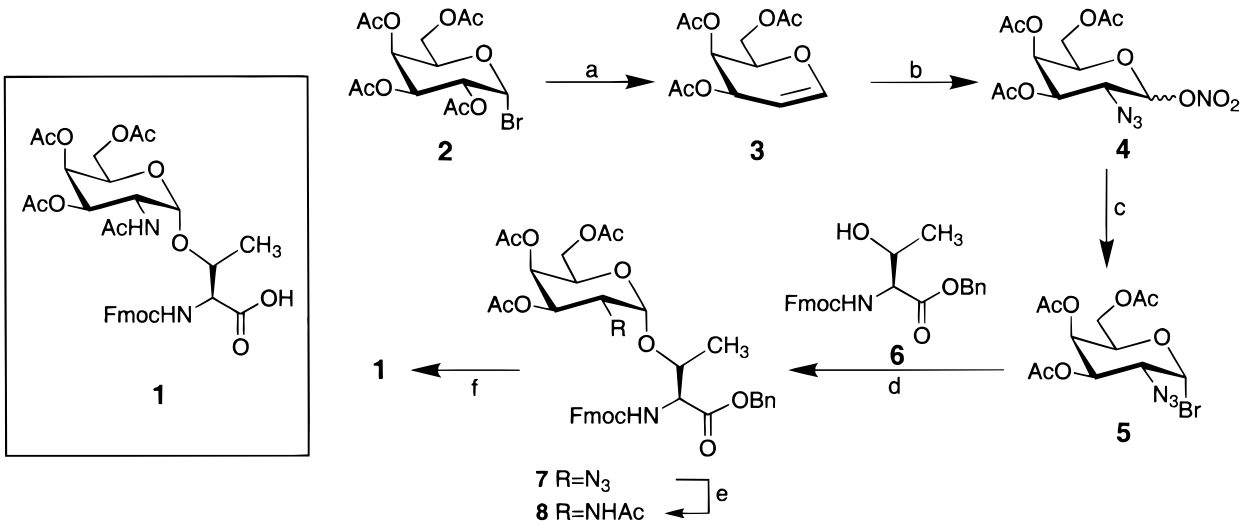

FIGURE 3: Synthetic scheme for Fmoc-Thr(Ac_3-α-D-GalNAc) (**1**). (a) Zn dust, AcOH/H_2O/ether. (b) Ceric ammonium nitrate, NaN_3, CH_3CN. (c) LiBr, CH_3CN. (d) Ag_2CO_3, $AgClO_4$, CH_2Cl_2/toluene. (e) Zn dust, THF/Ac_2O/AcOH, $CuSO_4$. (f) H_2, Pd/C, MeOH.

AcOH/H_2O/ether) afforded yields between 90 and 98% for this reaction, a significant improvement on previous methods[2] (*21*, *22*). The galactal could be taken on crude in an azidonitration reaction to afford compound **4** (*25*). Quantitative conversion to the azidobromide **5** yielded a coupling partner that could be reacted unpurified with Fmoc- and benzyl-protected threonine **6**. The desired α-glycoside **7** was obtained almost exclusively; trace amounts of the *β*-anomer were removed following reductive acetylation (**8**) by column chromatography. Thus, of the entire sequence, the only products requiring purification were **4** and **8**. Deprotection of the benzyl ester **8** by hydrogenolysis yielded the final product, N^{α}-Fmoc-Thr(Ac_3-α-D-GalNAc) (**1**), in a form pure enough for subsequent use. Protection of the threonine carboxylate as the *tert*-butyl ester worked equally well; in this case, deprotection by treatment with TFA afforded a final product requiring no purification.

Assembly of the peptides on solid phase was complicated by subtleties of the diptericin sequence. Diptericin contains the dipeptide unit Asp(45)-Asn(46), which is prone to an intramolecular cyclization reaction in which the backbone amide nitrogen of Asn attacks the protected *tert*-butyl ester of the Asp side chain (*33*). The product, an aspartimide, can be hydrolyzed to give a mixture of isomeric products. To circumvent the complications aspartimide formation could cause, we substituted Glu for Asp at position 45. The dipeptide unit Asp(29)-Gly(30) displays the same propensity for aspartimide formation; in this case, we precluded the side reaction by incorporating a glycine residue in which the α-NH_2 group was protected by a 2-hydroxy-4-methoxybenzyl group (*34*, *35*). Using these strategies, we successfully synthesized diptericin (Peptide 1) by the method described above. The peptide's identity was confirmed by electrospray mass spectrometry and its purity estimated by RP-HPLC analysis as 98% (Figure 4). The identities and purities of Peptides 2−6 were confirmed by the same methods (spectra not shown).

Circular Dichroism. Far-UV circular dichroism of full-length diptericin was used to probe for the presence of regular

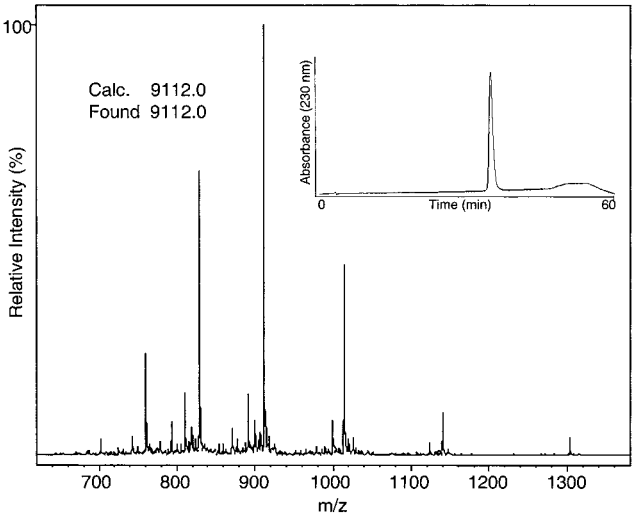

FIGURE 4: Electrospray mass spectrum and RP-HPLC trace (inset) of purified, full-length, glycosylated diptericin (Peptide 1). RP-HPLC elution was performed using a gradient of 10−50% acetonitrile in water (both containing 0.1% TFA) over 60 min.

secondary structure in the polypeptide. Spectra of unglycosylated full-length diptericin (Peptide 4) in 10 mM potassium phosphate buffer (pH 7.0) revealed a dramatic decrease in molar ellipticity at wavelengths approaching 200 nm, which is characteristic of peptides lacking a discrete conformational preference (Figure 5) (*36*). To test whether the peptide acquired structure in the presence of liposomes, as might be expected if it bound to lipid membranes, we recorded CD spectra in the presence of 1,2-dimyristoyl-sn-glycero-3-phosphocholine (a zwitterionic, neutral lipid) or 1,2-dimyristoyl-sn-glycero-3-phosphoglycerol (a negatively charged lipid); in each case, the peptide appeared unstructured (data not shown). These data are perhaps expected since a sequence such as diptericin's—rich in prolines and glycines—is poor in α-helical and *β*-strand propensity (*37*, *38*). Indeed, for both drosocin, a proline-rich peptide similar to diptericin's N-terminus, and attacin, a protein similar to the C-terminus (Figure 1), CD spectra reveal no evidence of regular structure unless the peptide is placed in a structure-inducing organic solvent (*13*, *39*). Since the activity of glycosylated diptericin

[2] An alternative, reportedly high yielding protocol for this reaction has been described by Broddefalk (*1*).

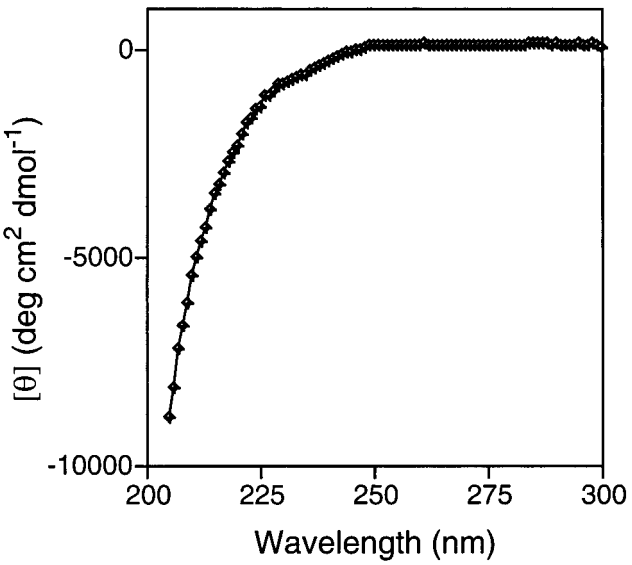

FIGURE 5: Far-UV CD spectrum of full-length, unglycosylated diptericin (Peptide 4, 6.0 μM) in 10 mM potassium phosphate (pH 7.0). The decline in molar ellipticity at wavelengths approaching 200 nm is characteristic of peptides lacking a defined structure. Identical spectra were obtained when the glycopeptide was incubated with liposomes of either 1,2-dimyristoyl-sn-glycero-3-phosphocholine or 1,2-dimyristoyl-sn-glycero-3-phosphoglycerol (data not shown). The spectrum shown represents the average of three scans.

was identical to that of its unglycosylated counterpart (Figure 6A), we hypothesized that it too would appear unstructured by CD; to conserve valuable glycopeptide, we chose to forego further CD experiments. A recent NMR study of drosocin did suggest that in an organic solvent, glycosylation is correlated with the induction of a turn structure in the vicinity of the carbohydrate (*40*). An analogous effect on the conformational dynamics of diptericin might be revealed via NMR analysis.

Growth Inhibition of E. coli D22. We tested the antibacterial potency of the chemically synthesized diptericin peptides by monitoring their ability to inhibit the growth of *E. coli*. Addition of full-length diptericin (Peptides 1 and 4) to a growing culture of D22 cells caused a decrease in growth rate. The antibacterial potencies of the glycosylated and unglycosylated versions were virtually identical (Figure 6A); both affected cell growth in two apparent phases, with a dramatic decrease (70%) between concentrations of 100 and 500 nM followed by a more gradual decline until complete inhibition was observed at a concentration of 10 μM. The approximate IC_{50} was 250 nM. This glycosylation independent activity contrasts with a previous report that the antibacterial capacity of diptericin isolated from *Phormia terranovae* larvae required the presence of at least one GalNAc residue (*5*).

To elucidate the functional roles of the proline-rich and attacin-like regions of the molecule, we tested the independent inhibitory activities of those fragments. The larger attacin-like fragment (Peptides 2 and 5) was itself an active antibiotic, albeit approximately 100-fold less potent than the parent molecule. A marked decrease in bacterial growth was observed at concentrations of peptide between 10 and 100 μM; here again, glycosylation did not significantly affect activity (Figure 6B). Interestingly, we observed a buckle in the dose response curve for these fragments; a moderate decrease in optical density (OD) of the bacterial culture between 2 and 10 μM was followed by a surprising increase in OD, which gave way to the marked decline at higher concentrations. Repeated experiments confirmed these basic results (data not shown); however, we did note more variability in this region of the dose response curve than at higher concentrations of peptide, which is reflected in the error bars of Figure 6B. A viable cell count experiment, shown in Figure 6C, revealed the same trend.

Fragments corresponding to the proline-rich region (Peptides 3 and 6) displayed no growth inhibitory activity at peptide concentrations up to 1 mM (data not shown). When these fragments were combined in 10 molar excess with the corresponding attacin-like fragments, no enhancement of antibacterial activity beyond that depicted in Figure 6B was seen (data not shown). Covalent attachment of the two regions was apparently a prerequisite of full antibacterial activity.

Effect on Outer Membrane Permeability. To evaluate possible alterations in outer membrane permeability in the presence of diptericin peptides, we cultured bacteria in the presence of a sublethal dose of peptide and then evaluated changes in the time course of bacterial growth upon addition of lysozyme. An intact outer membrane will normally serve as an effective barrier to lysozyme, impeding its access to the bacterial cell wall and thereby repressing its lytic effect (*41*). A culture of *E. coli* D22 grown in the presence of full-length diptericin (Peptide 1, 250 nM) displayed enhanced sensitivity to lysozyme. Addition of lysozyme caused an immediate reduction in OD; the bacteria were insensitive to lysozyme in the absence of diptericin (Figure 7A). This response mimics the effect seen when bacteria were grown in the presence of 100 nM polymyxin B, an antibiotic known to disrupt bacterial membranes (Figure 7B) (*41*, *42*). Similar behavior was seen for bacterial cultures exposed to the attacin-like fragment (Peptide 2), although higher concentrations of peptide (25 μM) were required (data not shown). Bacterial cultures containing the proline-rich fragment were unaffected by lysozyme addition (data not shown). In all cases, glycosylated peptides demonstrated the same activity as their unglycosylated counterparts.

Effect on Inner Membrane Permeability. To test the integrity of the bacterial inner membrane in the presence of diptericin, we used *E. coli* ML-35 cells, which express cytoplasmic β-galactosidase. We monitored uptake of an externally applied, chromogenic substrate, *o*-nitropheny-β-D-galactopyranoside (ONPG); disruption of the inner membrane permits cleavage of this normally excluded substrate by the cytoplasmic enzyme. Data were acquired using a peptide concentration of 1.0 μM, a 4-fold higher concentration of diptericin than was used in the outer membrane permeability assays. A control experiment in which the bacteria were exposed to polymyxin B (1.0 μM) delineates a positive response (Figure 8). Both full-length diptericin (Peptides 1 and 4, 1.0 μM) and the attacin-like fragment (Peptides 2 and 5, 1.0 μM) displayed enhanced inner membrane permeability versus a control culture (Figure 8). The parent molecule displayed heightened potency compared to the attacin-like fragment derived from it. The proline-rich fragment (Peptides 3 and 6, 1.0 μM) was inactive in these assays. In this experiment, as previously, no difference

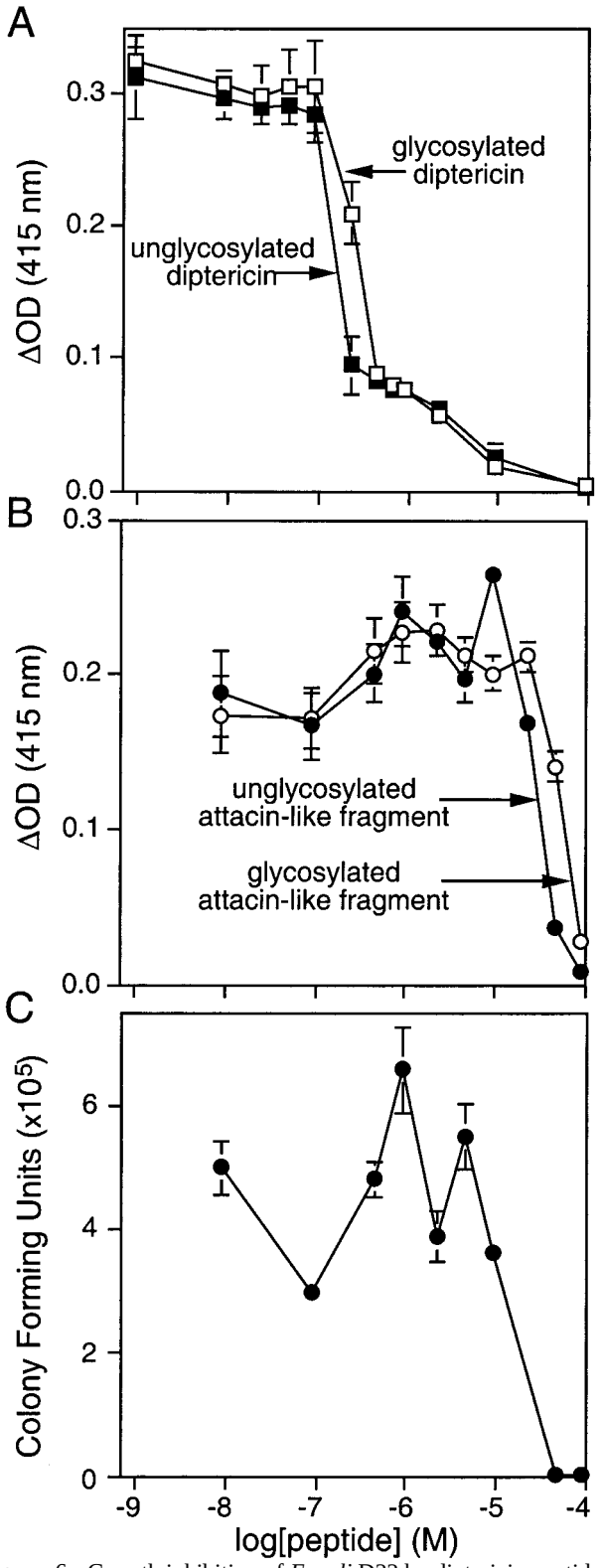

FIGURE 6: Growth inhibition of *E. coli* D22 by diptericin peptides. Serially diluted peptides (5 μL) were added to 50 μL of a dilute, growing bacterial culture; the combination was incubated at 25 °C for 24 h. Growth was monitored as the $\Delta OD_{415\ nm}$, or in the case of 6C, by counting the number of viable cells. (A) Full-length diptericin, glycosylated (□) and unglycosylated (■). (B) Attacin-like domain, glycosylated (○) and unglycosylated (●). (C) Viable cell count experiment, using samples withdrawn from the unglycosylated, attacin-like fragment experiment (●) shown in (B). Error bars represent standard deviation ($n = 3$) for (A) and (B), and high/low ($n = 2$) for (C). The proline-rich fragment of diptericin (glycosylated or unglycosylated) had no effect on bacterial growth in this assay (not shown).

between glycosylated and unglycosylated constructs was observed.

DISCUSSION

By pricking larvae of *Phormia terranovae* with an infected pin, one can trigger an immune reaction that loads their hemolymph with antibacterial peptides; diptericin, at a concentration estimated as 1 μg/mL (100 nM), is one component of this response (*14*). Refined measurements of diptericin's potency have been unavailable, presumably because the limited quantities isolated from insect hemolymph preclude such experiments. We report herein that chemically synthesized diptericin is active against *E. coli* D22 cells with an approximate IC_{50} of 250 nM. The similarity between this potency and the concentration of peptide in immune-challenged larvae suggests the exciting prospect that chemical synthesis can access the significant quantities of biologically active peptide necessary for a thorough structural and mechanistic study of diptericin. In addition, chemical methods facilitate fragment analysis and mutagenesis of the glycopeptide. Our preliminary work here narrows the major determinant of antibacterial activity to the C-terminal attacin-like portion of the molecule, illustrating this point.

While diptericin's mechanism is still enigmatic, our results provide some useful clues. Diptericin compromises the integrity of both the inner and outer membranes of *E. coli*. The access of a cytoplasmic enzyme, β-galactosidase, to a substrate in the surrounding media is enhanced in the presence of diptericin. Since the substrate, ONPG, is small enough to traverse pores in the outer membrane, the inner membrane is expected to be its major barrier to entry; cleavage of it by β-galactosidase suggests that this membrane is permeable. These findings are consistent with a previous study in which diptericin isolated directly from *P. terranovae* caused the release of cytoplasmic β-galactosidase from *E. coli* (*14*). Similarly, the access of lysozyme in the external media to its substrate, the peptidoglycan of the bacterial cell wall, is enhanced. At 14 000 Da, lysozyme is too large to pass through pores in the outer membrane (*41*, *43*, *44*), so the potency of its effect upon addition must be due to an increase in the outer membrane permeability mediated by diptericin.

Whether these membrane effects are diptericin's primary mode of action, or ancillary consequences, is unknown. We think it unlikely that the molecule functions primarily as a pore-former, binding with the membrane in a stoichiometric fashion and somehow opening channels in it. Peptides known to do so, such as the cecropins, tend to operate with equal facility on growing or stationary phase bacteria (*45*). Diptericin, in contrast, is active only on growing bacteria, a preference more indicative of a molecule that interrupts metabolic processes, such as protein, cell wall, or nucleic acid synthesis (*45*). In addition, circular dichroism spectroscopy indicated that diptericin lacked regular secondary structure in the presence of liposomes at lipid concentrations up to 3 mM (data not shown). The cecropins, which bind to lipids professionally, acquire secondary structure in the presence of liposomes or hydrophobic solvents (*46*, *47*). Finally, peptides that lack a specific bacterial target and instead bind to membranes are expected to be equally potent as the all D-amino acid enantiomer; this hypothesis was born

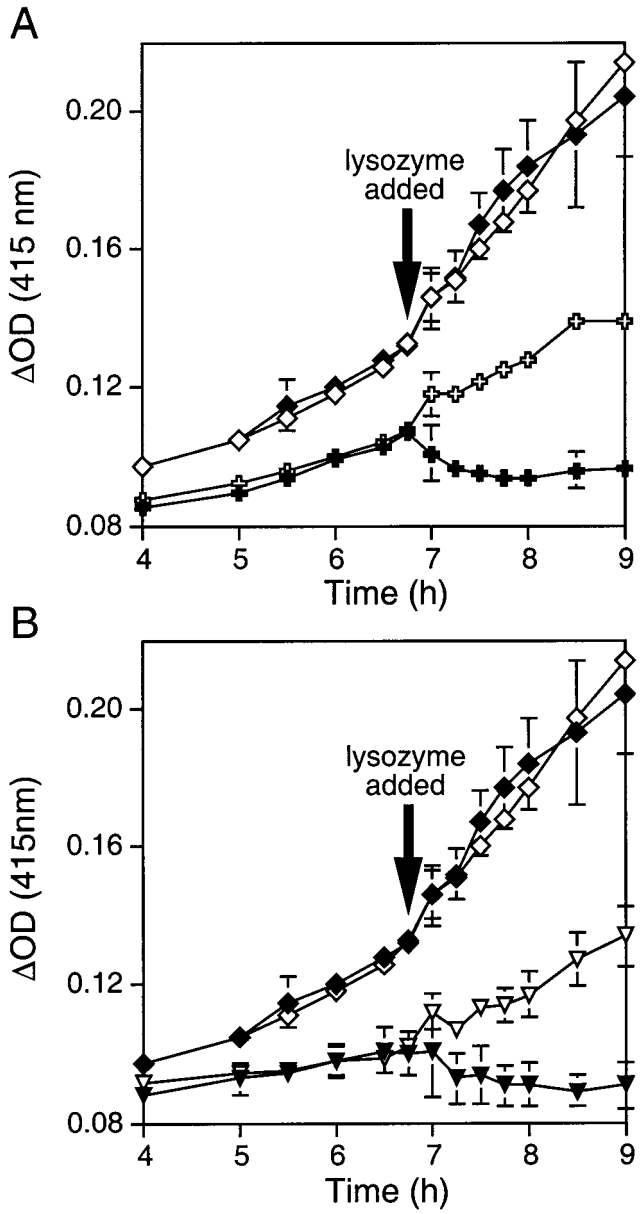

FIGURE 7: Effect of diptericin on bacterial outer membrane permeability. At the time indicated by the arrow, lysozyme (final concentration 0.2 mg/mL) was added to a growing culture of *E. coli* D22 containing full-length, glycosylated diptericin (0.25 μM) (solid cross). The immediate reduction in $OD_{415\ nm}$ upon lysozyme addition suggests that the permeability of the bacterial outer membrane is enhanced in the presence of diptericin, allowing access of lysozyme to its substrate, the peptidoglycan of the bacterial cell wall. Control cultures shown: diptericin only (open cross), lysozyme only (◆), and no additions (◇). Identical results were observed for the unglycosylated, full-length peptide (not shown). The same results were observed with the attacin-like fragment (glycosylated or unglycosylated), although 100-fold higher peptide concentrations (25 μM) were required (not shown). The proline-rich domains, glycosylated and unglycosylated, were inactive in this assay (not shown). (B) A control experiment showing the effect of 0.10 μM polymyxin B on outer membrane permeability. This antibiotic, known to act by compromising membrane integrity, effected the same reduction in $OD_{415\ nm}$ upon addition of lysozyme (▼, final concentration 0.2 mg/mL) as did diptericin. Control cultures shown: polymyxin B only (▽), lysozyme only (◆), and no additions (◇). For all experiments, error bars represent standard deviation ($n = 3$).

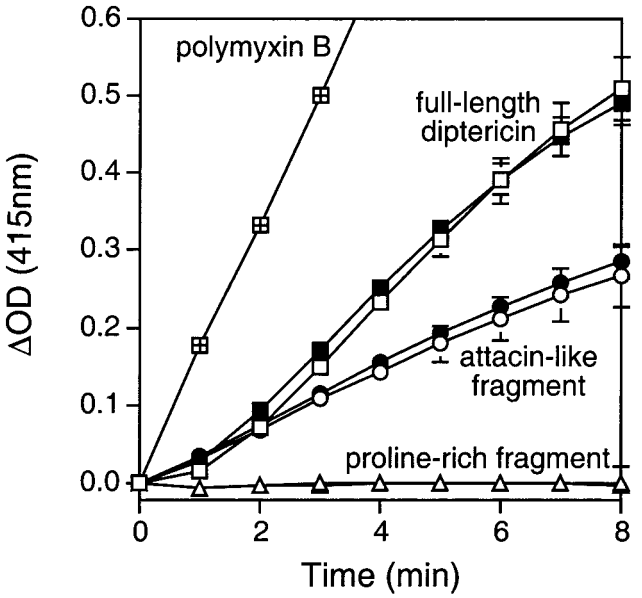

FIGURE 8: Effect of diptericin on bacterial inner membrane permeability. *E. coli* ML-35 cells, which express cytoplasmic β-galactosidase, were added to a solution containing ONPG, a substrate for that enzyme. Diptericin constructs were added at a final concentration of 1 μM, and the production of *o*-nitrophenolate was monitored at $OD_{415\ nm}$. An increased $OD_{415\ nm}$, representing enhanced access of the enzyme to its substrate, suggests that the bacterial inner membrane has been disrupted. Results for the following peptides are shown: polymyxin B, a positive control (⊞); full-length diptericin, glycosylated (□) and unglycosylated (■); the attacin-like domain, glycosylated (○) and unglycosylated (●); the proline-rich domain, glycosylated (△) and unglycosylated (▲). For all experiments, error bars represent standard deviation ($n = 3$).

out for cecropin (*46*). Yet the enantiomers of two proline-rich peptides similar to diptericin's N-terminus, drosocin and apidaecin, were either inactive or dramatically less potent (*12*, *13*).

These observations suggest that diptericin may function more akin to its phylogenetic cousin, attacin, which increases membrane permeability as a byproduct of its inhibition of outer membrane protein synthesis (*9*, *10*). The bacterial targets of the two peptides may or may not be the same. From a strategic perspective, it would be in the insect's interest to maximize the antibacterial range of its immune system by diversifying the bacterial targets of immune peptides. In addition, considering the N-terminal proline-rich appendage of diptericin that is lacking in attacin, we might expect some differences in targeting and mechanism. An engaging recent paper suggests that attacin can exert its effect on outer membrane protein synthesis without entering the bacterial cell (*11*); studies of this type have not yet been performed on diptericin. Conversely, while a previous study of diptericin identified an inhibition of amino acid transport as the earliest measured effect of diptericin (*14*), similar effects have not been reported for attacin. We look forward to probing more fully how the activities of attacin and diptericin compare.

Our analysis of diptericin's putative domains suggests that the attacin-like region contains the major determinants of the molecule's antibacterial activity. This fragment exhibited a profile of activity similar to, although 100-fold less potent than, the full-length peptide. The proline-rich region was devoid of activity in all our assays. We were intrigued by the undulations in the dose response curve for the attacin-like fragment; this behavior represented the only qualitative

difference between this fragment's activity and that of the parent molecule. Ongoing experiments in the lab seek to characterize the condition of bacteria at different points along the dose response curve and to understand how addition of the proline-rich region curtails this behavior. While it would be premature to interpret heavily this preliminary fragment analysis, we hope that future experiments will clarify whether the two regions of the molecule can indeed be described as functionally separate domains.

We were surprised to observe that diptericin's activity was consistently independent of its glycosylation state. In a previous report by Bulet et al., glycopeptide isolated from *Phormia terranovae* larvae was determined to be inactive after enzymatic removal of the carbohydrates (*5*). Possibly, subtle growth inhibition by the deglycosylated peptide went undetected in that study; in our hands, the solid agar assay used by Bulet is approximately 100-fold less sensitive than the liquid culture assay we typically employ. It remains possible that the diptericin glycoform bearing disaccharides at each site—as opposed to the monosaccharides we installed—would be markedly more active than other isoforms; data from the previous study suggests some enhancement of activity in this glycoform. It is also possible that glycosylation is simply not as relevant to antibacterial potency as we had anticipated. A homologue in *S. peregrina* exists unmodified, and one in *D. melanogaster*, while not yet characterized in this regard, is at the least missing the requisite serine or threonine residue at position 54 (*48*, *49*).

Glycosylation's role in this corner of insect immunity thus remains an unanswered question. Carbohydrates decorate a number of proline-rich peptides homologous to the N-terminus of diptericin (Figure 1). While glycosylation enhances the activity of drosocin, formaecin, and an additional proline-rich peptide, lebocin (*6*, *7*, *50*), it appears neutral with respect to pyrrhocoricin (our unpublished data). Carbohydrate addition may be a phylogenetic artifact in some peptides or it may mediate a process our assays do not measure; other posttranslational modifications, such as C-terminal amidation, modulate the range of bacteria against which some antimicrobial peptides are active (*51*, *52*). Further, glycosylation of mammalian proteins is known to modulate serum half-life and provide specific clearance mechanisms, properties that would only be evident in an intact organism (*53*). We plan to probe these possibilities.

Ultimately, to understand the mechanism of diptericin, we must identify its bacterial target(s). The ability to chemically synthesize the peptide in its different isoforms enables us to approach this question for the first time. We see the experiments reported herein as the prelude to a fruitful course of study.

ACKNOWLEDGMENT

We are grateful to Professor Robert E. W. Hancock of the University of British Columbia for providing the *E. coli* ML-35 cells used in the inner membrane permeability assay and to Dr. Mary Berlyn of the *E. coli* Genetic Stock Center at Yale University for the *E. coli* D22 cells used in the other antibacterial assays. We thank Professor Susan Marqusee for the use of her CD spectrometer and Julie Hollien for assistance with those experiments. We are grateful to Professor Majendra Jain for his insight on antibacterial experiments. Several people in our laboratory have helped develop the synthesis of N^{α}-Fmoc-Thr(Ac_3-α-D-GalNAc); we thank Elena Rodriguez, Lisa Marcaurelle, Scarlett Goon, and Dr. Youngsook Shin for their contributions. Finally, we are indebted to Dr. J. Mark Quillan and Joshua I. Armstrong for their advice on many aspects of the project.

REFERENCES

1. Broddefalk, J., Nilsson, U., and Kihlberg, J. (1994) *J. Carbohydr. Chem. 13*, 129−132.
2. Hultmark, D. (1993) *Trends Genetics 9*, 178−83.
3. Boman, H. G., and Hultmark, D. (1987) *Annu. Rev. Microbiol. 41*, 103−26.
4. Piers, K. L., and Hancock, R. E. (1994) *Mol. Microbiol. 12*, 951−8.
5. Bulet, P., Hegy, G., Lambert, J., Van Dorsselaer, A., Hoffmann, J. A., and Hetru, C. (1995) *Biochemistry 34*, 7394−400.
6. Bulet, P., Dimarcq, J. L., Hetru, C., Lagueux, M., Charlet, M., Hegy, G., Van Dorsselaer, A., and Hoffmann, J. A. (1993) *J. Biol. Chem. 268*, 14893−7.
7. Hara, S., and Yamakawa, M. (1995) *Biochem. J. 310*, 651−6.
8. Bulet, P. (1999) *Medicine/Sciences 15*, 23−9.
9. Engström, P., Carlsson, A., Engström, Å., Tao, Z.-j., and Bennich, H. (1984) *EMBO J. 3*, 3347−51.
10. Carlsson, A., Engström, P., Palva, E. T., and Bennich, H. (1991) *Infect. Immun. 59*, 3040−5.
11. Carlsson, A., Nyström, T., de Cock, H., and Bennich, H. (1998) *Microbiol. 144*, 2179−88.
12. Casteels, P., and Tempst, P. (1994) *Biochem. Biophys. Res. Commun. 199*, 339−45.
13. Bulet, P., Urge, L., Ohresser, S., Hetru, C., and Otvos, L., Jr. (1996) *Eur. J. Biochem. 238*, 64−9.
14. Keppi, E., Pugsley, A. P., Lambert, J., Wicker, C., Dimarcq, J., Hoffmann, J. A., and Hoffmann, D. (1989) *Arch. Insect Biochem. Physiol. 10*, 229−239.
15. Kuduk, S. D., Schwarz, J. B., Chen, X. T., Glunz, P. W., Sames, D., Ragupathi, G., Livingston, P. O., and Danishefsky, S. J. (1998) *J. Am. Chem. Soc. 120*, 12474−12485.
16. Sames, D., Chen, X. T., and Danishefsky, S. J. (1997) *Nature 389*, 587−91.
17. Klich, G., Paulsen, H., Meyer, B., Meldal, M., and Bock, K. (1997) *Carbohydr. Res. 299*, 33−48.
18. Andreotti, A. H., and Kahne, D. (1993) *J. Am. Chem. Soc. 115*, 3352−3353.
19. Paulsen, H., and Adermann, K. (1989) *Liebigs Ann. Chem.*, 751−769.
20. Szabó, L., Ramza, J., Langdon, C., and Polt, R. (1995) *Carbohydr. Res. 274*, 11−28.
21. Shull, B. K., Wu, Z. J., and Koreeda, M. (1996) *J. Carbohydr. Chem. 15*, 955−964.
22. Shafizadeh, F. (1963) *Methods Carbohydr. Chem. 2*, 409−410.
23. Barnett, J. E. (1967) *Adv. Carbohydr. Chem. Biochem. 22*, 177−227.
24. Higashi, K., Nakayama, K., Shioya, E., and Kusama, T. (1991) *Chem. Pharm. Bull. 39*, 2502−2504.
25. Lemieux, R. U., and Ratcliffe, R. M. (1979) *Can. J. Chem. 57*, 1244−1251.
26. Kunz, H., Birnbach, S., and Wernig, P. (1990) *Carbohydr. Res. 202*, 207−223.
27. Chang, C. D., Waki, M., Ahmad, M., Meienhofer, J., Lundell, E. O., and Haug, J. D. (1980) *Int. J. Peptide Prot. Res. 15*, 59−66.
28. King, D. S., Fields, C. G., and Fields, G. B. (1990) *Int. J. Peptide Prot. Res. 36*, 255−66.
29. Pace, C. N., Vajdos, F., Fee, L., Grimsley, G., and Gray, T. (1995) *Protein Sci. 4*, 2411−23.
30. Falla, T. J., and Hancock, R. E. W. (1997) *Antimicrob. Agents Chemother. 41*, 771−5.

31. Satyanarayana, J., Gururaja, T. L., Naganagowda, G. A., Ramasubbu, N., and Levine, M. J. (1998) *J. Peptide Res. 52*, 165−79.
32. Kunz, H. (1996) in *Preparative Carbohydrate Chemistry* (Hanessian, S., Ed.) pp 265−281, Marcel Dekker, Inc., New York.
33. Yang, Y., Sweeney, W. V., Schneider, K., Thörnqvist, S., Chait, B. T., and Tam, J. P. (1994) *Tetrahedron Lett. 35*, 9689−9692.
34. Quibell, M., Owen, D., Packman, L. C., and Johnson, T. (1994) *J. Chem. Soc., Chem. Commun.*, 2343−2344.
35. Packman, L. C. (1995) *Tetrahedron Lett. 36*, 7523−7526.
36. Woody, R. W. (1996) in *Circular dichroism and the conformational analysis of biomolecules* (Fasman, G. D., Ed.) pp 25−67, Plenum, New York.
37. O'Neil, K. T., and DeGrado, W. F. (1990) *Science 250*, 646−51.
38. Kim, C. A., and Berg, J. M. (1993) *Nature 362*, 267−70.
39. Gunne, H., Hellers, M., and Steiner, H. (1990) *Eur. J. Biochem. 187*, 699−703.
40. McManus, A. M., Otvos, L., Jr., Hoffmann, R., and Craik, D. J. (1999) *Biochemistry 38*, 705−14.
41. Hancock, R. E., and Wong, P. G. (1984) *Antimicrob. Agents Chemother. 26*, 48−52.
42. Hancock, R. E. (1984) *Annu. Rev. Microbiol. 38*, 237−64.
43. Nikaido, H., and Vaara, M. (1985) *Microbiol. Rev. 49*, 1−32.
44. Hancock, R. E. W. (1987) *J. Bacteriol. 169*, 929−33.
45. Boman, H. G., Agerberth, B., and Boman, A. (1993) *Infect. Immun. 61*, 2978−84.
46. Wade, D., Boman, A., Wahlin, B., Drain, C. M., Andreu, D., Boman, H. G., and Merrifield, R. B. (1990) *Proc. Natl. Acad. Sci. U.S.A. 87*, 4761−5.
47. Mancheño, J. M., Oñaderra, M., Martínez del Pozo, A., Díaz-Achirica, P., Andreu, D., Rivas, L., and Gavilanes, J. G. (1996) *Biochemistry 35*, 9892−9.
48. Ishikawa, M., Kubo, T., and Natori, S. (1992) *Biochem. J. 287*, 573−8.
49. Wicker, C., Reichhart, J. M., Hoffmann, D., Hultmark, D., Samakovlis, C., and Hoffmann, J. A. (1990) *J. Biol. Chem. 265*, 22493−8.
50. Mackintosh, J. A., Veal, D. A., Beattie, A. J., and Gooley, A. A. (1998) *J. Biol. Chem. 273*, 6139−43.
51. Lee, J. Y., Boman, A., Sun, C. X., Andersson, M., Jörnvall, H., Mutt, V., and Boman, H. G. (1989) *Proc. Natl. Acad. Sci. U.S.A. 86*, 9159−62.
52. Callaway, J. E., Lai, J., Haselbeck, B., Baltaian, M., Bonnesen, S. P., Weickmann, J., Wilcox, G., and Lei, S. P. (1993) *Antimicrob. Agents Chemother. 37*, 1614−9.
53. Cumming, D. A. (1991) *Glycobiol. 1*, 115−30.
54. Engström, Å., Engström, P., Tao, Z.-j., Carlsson, A., and Bennich, H. (1984) *EMBO J. 3*, 2065−2070.
55. Kockum, K., Faye, I., von Hofsten, P., Lee, J.-Y., Xanthopoulos, K. G., and Boman, H. G. (1984) *EMBO J. 3*, 2071−2075.
56. Ando, K., Okada, M., and Natori, S. (1987) *Biochemistry 26*, 226−30.
57. Cociancich, S., Dupont, A., Hegy, G., Lanot, R., Holder, F., Hetru, C., Hoffmann, J. A., and Bulet, P. (1994) *Biochem. J. 300*, 567−75.
58. Casteels, P., Ampe, C., Jacobs, F., Vaeck, M., and Tempst, P. (1989) *EMBO J. 8*, 2387−91.

BI991247F